scientific reports

Check for updates

OPEN

Prognostic significance and response to immune checkpoint inhibitors of RIPK3, MLKL and necroptosis in non-small cell lung cancer

Nattaya Duangthim[1], Thanpisit Lomphithak[7], Ryoko Saito-Koyama[2,3], Yasuhiro Miki[2], Chihiro Inoue[2], Ikuro Sato[4], Eisaku Miyauchi[5], Jiro Abe[6], Hironobu Sasano[2] & Siriporn Jitkaew[7,8]✉

Lung cancer remains the leading cause of cancer death. Treatment with immune checkpoint inhibitor (ICI) alone or combination with chemotherapy served as first-line therapy in non-small cell lung cancer (NSCLC). However, only 20–50% of NSCLC patients respond to ICI. Necroptosis, an inflammatory form of cell death plays an important role in the regulation of tumor immune microenvironment which may affect prognosis and ICI response but its clinical significance in NSCLC patients has remained largely unknown. Therefore, we aimed to analyze the correlation between key necroptotic proteins and necroptosis and clinical outcomes, the status of tumor-infiltrating immune cells, and response to ICI in NSCLC patients. The expression of receptor-interacting protein kinase 3 (RIPK3), mixed lineage kinase domain-like protein (MLKL) and phosphorylated MLKL (pMLKL) were immunolocalized in 125 surgically resected NSCLC patients and 23 NSCLC patients administered with ICI therapy. CD8 + and FOXp3 + T cells and CD163 + M2 macrophages were also immunolocalized. High RIPK3 status was positively correlated with survival of the patients and RIPK3 turned out an independent favorable prognostic factor of the patients. RIPK3 was negatively correlated with CD8 + T cells, while MLKL positively correlated with CD163 + M2 macrophages, suggesting the possible involvement of RIPK3 and MLKL in formulating immunosuppressive microenvironment. In addition, high RIPK3 status tended to be associated with clinical resistance to ICI therapy (*P*-value = 0.057). Furthermore, NSCLC cells-expressing RIPK3 suppressed T cells response to ICI therapy in vitro. Therefore, RIPK3 and MLKL could induce an immunosuppressive microenvironment, resulting in low response to ICI therapy in NSCLC.

Keywords Immune checkpoint inhibitor, Immune microenvironment, Necroptosis, Non-small cell lung cancer, Receptor-interacting protein kinase 3

Abbreviations

CR	Complete response
ICI	Immune checkpoint inhibitor

[1]Graduate Program in Clinical Biochemistry and Molecular Medicine, Department of Clinical Chemistry, Faculty of Allied Health Sciences, Chulalongkorn University, Bangkok 10330, Thailand. [2]Department of Pathology, Tohoku University School of Medicine, Sendai, Miyagi 980-8575, Japan. [3]Department of Pathology, National Hospital Organization, Sendai Medical Center, Sendai, Miyagi 980-8575, Japan. [4]Department of Pathology, Miyagi Prefectural Cancer Center, Natori, Miyagi 981-1293, Japan. [5]Department of Respiratory Medicine, Tohoku University Hospital, Sendai, Miyagi 980-8575, Japan. [6]Department of Thoracic Surgery, Miyagi Cancer Center, Natori, Miyagi 981-1293, Japan. [7]Department of Clinical Chemistry, Faculty of Allied Health Sciences, Chulalongkorn University, Bangkok 10330, Thailand. [8]Center of Excellence for Cancer and Inflammation, Department of Clinical Chemistry, Faculty of Allied Health Sciences, Chulalongkorn University, Bangkok 10330, Thailand. ✉email: Siriporn.Ji@chula.ac.th

IHC	Immunohistochemical
LUAD	Lung adenocarcinoma
LUSC	Lung squamous cell carcinoma
MLKL	Mixed lineage kinase domain-like
NSCLC	Non-small cell lung cancer
OS	Overall survival
PD	Progressive disease
PD-L1	Programmed death-ligand 1
pMLKL	Phosphorylated mixed lineage kinase domain-like
PR	Partial response
RIPK3	Receptor-interacting protein kinase 3
SD	Stable disease
TME	Tumor microenvironment

Lung cancer is the leading causes of cancer-related death worldwide, approximately 1.8 million deaths in 2020[1]. The most common type of lung cancer is non-small cell lung cancer (NSCLC), which accounts for 85% of all cases[2]. The 5-year survival rate of NSCLC patients is less than 20% due to the lack of early diagnosis and effective therapy[3]. Recently, treatment with immune checkpoint inhibitor (ICI) alone or combination with chemotherapy was established as first-line therapy in NSCLC[4]. Analysis of programmed death-ligand 1 (PD-L1) expression in tumor cells using immunohistochemistry is currently the U.S. Food and Drug Administration (FDA)-approved predictive biomarker used for the selection of NSCLC patient who may respond to ICI[5]. However, among those selected by PD-L1 immunohistochemistry, only 20–50% clinically respond to ICI[6]. Therefore, it has become pivotal to explore more effective biomarkers for predicting prognosis and ICI response in NSCLC.

Increasing evidence has revealed that tumor-infiltrating immune cells (TIICs) such as CD4 + or CD8 + T cells, regulatory T (Treg) cells, and tumor-associated macrophages (TAMs; M2 macrophages) could be important factors that influence clinical response to ICI therapy[7–9]. In NSCLC, high infiltration of CD8 + T cells, a major type of immune cells in anti-tumor immunity, in the tumor tissues, was reported to be significantly correlated with clinical response to ICI therapy[10,11]. However, M2 macrophages were reported to be associated with resistance to ICI therapy[12]. Accumulating evidence suggests the interplay or possible crosstalk between TIICs and tumor cell death in tumor microenvironment (TME)[13,14]. Therefore, the analysis of TIICs and cell death markers is considered indispensable for predicting prognosis, clinical outcomes and response to therapy in NSCLC.

Necroptosis, a regulated form of necrosis and caspase-independent cell death, has been considered as an inflammatory cell death. Receptor-interacting protein kinase 1 (RIPK1), receptor-interacting protein kinase 3 (RIPK3) and mixed lineage kinase domain-like protein (MLKL) are all key components in necroptosis pathway[15–20]. Upon the activation of necroptosis, RIPK1, RIPK3 and MLKL were recruited to form a necrosome complex. In the necrosome, RIPK3 phosphorylates MLKL, subsequently resulting in MLKL oligomerization and translocation of MLKL into plasma membrane where oligomerized MLKL disrupts permeability of plasma membrane[21]. The rupture of the plasma membrane leads to the release of intracellular contents including damage-associated molecular patterns (DAMPs) and inflammatory cytokines/chemokines into TME, creating an inflammatory TME[22].

Necroptosis and key necroptotic proteins have been reported to play a double-edged sword role (i.e. tumor promotion and suppression) in cancers[23,24]. On the one hand, key necroptotic proteins were downregulated and associated with poor prognosis in various human malignancies suggesting a tumor suppressive role of necroptosis[25–30], although the underlying mechanisms have remained elusive[31,32]. In addition, necroptosis could also evoke marked inflammatory and immune responses which could enhance anti-tumor immunity and tumor suppression and therefore therapy-induced necroptosis was proposed as a novel cancer therapy[24]. On the other hand, several studies also reported that tumor cell necroptosis promoted cancer development, progression and immunosuppression[33]. Upregulation of key necroptotic factors was reported to be associated with an unfavorable prognosis in esophageal squamous cell carcinoma (ESCC), head and neck squamous cell carcinoma (HNSCC), low-grade glioma (LGG) and glioblastoma multiforme (GBM) primary tissues[34–36]. In addition, RIPK3-mediated necroptosis has been reported to create immunosuppressive TME by enhancing CD163 + M2 macrophages and myeloid-derived suppressor cells (MDSCs) infiltration through the release of CXCL1 and SAP130 chemokines in a pancreatic ductal adenocarcinoma (PDA) mouse model[37]. A study in cholangiocarcinoma (CCA) tissues demonstrated that MLKL status in tumor cells was significantly negatively correlated with CD8 + T cells, while positively correlated with CD163 + M2 macrophages[38]. In addition, necroptosis was also reported to be associated with radiation-induced tumor cell repopulation and recurrence in colorectal cancer[39]. A recent study demonstrated a negative correlation between pMLKL and CD8 + T cells in ESCC, resulting in a decreased response of neoadjuvant chemotherapy (NAC)[34]. However, the clinical and prognostic significance of necroptosis and key necroptotic proteins in NSCLC have largely unknown.

Therefore, in this study, we first immunolocalized several key markers related to necroptosis and TIICs in 125 surgically resected NSCLC cases and 23 NSCLC patients who received ICI therapy as the first-line therapy. We then analyzed the correlation between the status of key necroptotic proteins and necroptosis itself and clinical outcomes, TIICs and response to ICI in these cases. Moreover, in vitro co-culture between NSCLC cells-expressing RIPK3 with primary human T cells was conducted to evaluate the responsiveness to ICI therapy. This is the first study to provide systemic analysis of necroptosis and TIICs in TME and ICI response in NSCLC which might lead to a better understanding of necroptosis and provide potential prognostic and predictive biomarkers for NSCLC patients.

Materials and methods

Patient selection and clinical data collection

The tissue specimens of NSCLC were obtained from 125 patients who underwent surgery resection at Miyagi Cancer Center, Miyagi, Japan between 2014 to 2015. None of the patients received any chemotherapy or radiation before surgery. This cohort consists of two subtypes, 95 cases of lung adenocarcinoma (LUAD) and 30 cases of lung squamous cell carcinoma (LUSC). Clinicopathological factors of each patient were summarized in Table S1. Additional 23 NSCLC patients who received ICI therapy as the first-line therapy were also recruited in this study in order to explore the correlation between necroptosis and clinical response to ICI therapy. Biopsy specimens of these 23 cases were obtained from Tohoku University Hospital, Miyagi, Japan between 2017 to 2019 prior to the administration of ICI therapy. All 23 cases were associated with relatively abundant PD-L1 immunoreactivity (the total proportion score: > 50%) according to KEYNOTE-024 (ClinicalTrials. gov, NCT02142738) and were subsequently treated with anti-PD-1 (pembrolizumab) in combination with chemotherapy according to the pathological diagnosis. The therapeutic efficacy in those cases above were tentatively determined according to the Response Evaluation Criteria in Solid Tumours (RECIST) version 1.1.16. In this study, patients who achieved a complete response (CR) or partial response (PR) were classified as responders, while stable disease (SD) and progressive disease (PD) were classified as non-responders. All the tissue specimens were fixed in 10% neutral formalin and embedded in paraffin. The study protocol was approved by the Ethics Committee at the Tohoku University School of Medicine.

Immunohistochemical (IHC) staining

Tissue sections were deparaffined and rehydrated in absolute xylene and ethanol, respectively. Antigen retrieval was performed by autoclaving the slides for 5 min at 121 °C in antigen retrieval solution (sodium citrate buffer, pH 6.0 for RIPK3, CD8, CD163 and FOXp3; sodium citrate buffer, pH 9.0 for MLKL and pMLKL). After blocking non-specific binding using a blocking solution provided (Histofine Kit; Nichirei Bioscience, Japan), tissue sections were incubated overnight at 4 °C with primary antibodies including anti-RIPK3 (ab72106; Abcam, Cambridge, UK; 1:800), anti-MLKL (ab184718; 1:2000), anti-pMLKL (ab187091; 1:200), anti-FOXp3 (ab20034; 1:200), anti-CD8 (Dako, Glostrup, Denmark; 1:50) and anti-CD163 (NCL-L-CD163; Leica Biosystems, Wetzlar, Germany; 1:600). The Dako PD-L1 22C3 pharmDx kit (Dako, Carpinteria, CA) on the Dako Link 48 platform was used for PD-L1 staining. Endogenous peroxide activity was then blocked with methanol containing 0.5% hydrogen peroxidase. Subsequently, the sections were incubated with a biotin-streptavidin horseradish peroxidase-conjugated secondary antibody (Histofine Kit; Nichirei Bioscience, Japan) at room temperature for 1 h for RIPK3, CD8, CD163 and FOXp3, while MLKL and pMLKL were incubated with HRP-polymer secondary antibodies (EnVision kit; Dako, Agilent Technologies, Inc., Santa Clara, CA, USA). After that, antigen–antibody complexes were visualized by 3,3′-diaminobenzidine (DAB) solution (1 mM DAB, 50 mM Tris–HCL buffer, pH 7.6 and 0.006% H_2O_2) and counterstained with haematoxylin. Non pathological kidney tissues obtained from autopsy were used as a positive control for RIPK3, while non pathological tonsil tissues served as a positive control for MLKL, CD8, CD163 and FOXp3. Macrophages were used as a positive control for PD-L1 in all the tissues examined. Based on a previous study, HT-29 colon carcinoma cells treated with TNF-α/Smac mimetic/zVAD-fmk (TSZ) and untreated HT-29 paraffin-embedded cell blocks, were used as positive and negative controls for pMLKL, respectively[38].

Evaluation of immunoreactivity

Immunoreactivity was evaluated in the whole tissue sections of all biopsy cases. The cells were tentatively determined positive when the cells had higher immunoreactivity intensity than the background. Modified H-score was used to assess the relative immunointensity of RIPK3, MLKL and PD-L1. Briefly, the intensity was divided into three groups: negative, weak and strong and the modified H-score was calculated using the following formula: (%Strong × 2) + (%Weak × 1), giving a possible range 0–200. As the number of pMLKL positive cells was only a few cells and there were no significant differences in the relative immunointensity in individual positive cells. Therefore, immunoreactivity of pMLKL was tentatively divided into the following two groups: negative and positive for pMLKL. In order to evaluate the number of CD8 + and FOXp3 + T cells and CD163 + M2 macrophages, the positive cells located in two different locations in each tumor tissues were counted including intratumoral compartment (within the tumor cell nests) and within the adjacent stroma (immune cells within one tumor cell diameter of the tumor) following a previous report[40]. In addition, the positive cells in five fields with high numbers of TIICs (hot spots) were counted and averaged the five counts (Fig. S1). All specimens were evaluated by two authors (N.D and R.S, a board-certified pathologist).

Bioinformatic analysis

TISIDB (http://cis.hku.hk/TISIDB), an Integrated Tumor-Immune System Interaction Repository which integrated multiple types of data resources in onco-immunology, was used to validate the correlation between key necroptotic factors and ICI therapeutic response. This study used immunotherapy modes, collected the genomic profiles of pre-treatment tumor biopsies from responders and non-responders treated with immunotherapy in several public studies. The expression difference of interested gene between responder and non-responder groups in various studies was represented in a volcano plot. Each of red circle in the volcano plot represents each of the study, more detail of each study could be obtained by searching PubMed PMID in TISIDB[41].

Cell culture

Human NSCLC cell lines A549, HCC827, and H1975 were obtained from ATCC. All cell lines were cultured in RPMI medium (Cytiva Life Sciences, Marlborough, MA, USA) supplemented with 10% fetal bovine serum (Sigma, St. Louis, MO, USA) and 1% Penicillin–Streptomycin (Cytiva Life Sciences, Marlborough, MA, USA).

The cell lines were maintained in a humidified incubator at 37 °C with 5% CO_2. Additionally, rigorous testing confirmed the absence of mycoplasma contamination in any of the cell lines.

Western blot analysis

The cells were washed twice with ice-cold PBS and then lysed in RIPA buffer (Merck Millipore, Darmstadt, Germany) supplemented with a proteinase inhibitor cocktail (Roche, Mannheim, Germany) on ice for 30 min. Total protein concentrations were determined using the Bradford assay (Bio-Rad, Hercules, CA, USA). Subsequently, total proteins (25 µg) were separated using 10–20% SDS-PAGE and transferred onto PVDF membranes. The membranes were blocked with a 5% blotting-grade blocker (Bio-Rad, Hercules, CA, USA) at room temperature for 1 h, followed by overnight incubation with primary antibodies at 4 °C. The primary antibodies employed in this study were anti-RIPK3 (8457), anti-PD-L1 (E1L3N®) (13,684), and anti-β-Actin (4970) from Cell Signaling (Danvers, MA, USA). After incubation with primary antibodies, the blots were washed three times with TBS-T (Tris-buffered saline, 0.5% Tween 20) buffer and incubated with horseradish peroxidase-conjugated secondary antibodies (Cell Signaling Technology, Danvers, MA, USA) at room temperature for 1 h. Protein bands were visualized using enhanced chemiluminescence following the manufacturer's instructions (Bio-Rad, Hercules, CA, USA) with Amersham ImageQuant 800 Western blot imaging systems (Cytiva Life Sciences, Marlborough, MA, USA). All Western blots presented are representative of a minimum of three independent experiments.

Generation of NSCLC cell lines overexpressing RIPK3

The Lentiviral vector pLESIP-RIPK3 was generated by subcloning human RIPK3 (NM_006871) into pLESIP from RIPK3-EGFP construct, which was kindly provided by Dr. Francis Ka Ming Chan (University of Massachusetts Medical School). All plasmid constructs were verified through DNA sequencing. To generate lentiviral particles, HEK293T cells were co-transfected with the packaging plasmid (pCMV-VSV-G) and the envelope plasmid (pCMV-dr8.2-dvpr), along with either the pLESIP empty vector or the pLESIP-RIPK3 vector. After 24 h, supernatants were collected and filtered through a 0.45 µm sterile filter membrane (Jet Bio-Filtration, Guangzhou, China) to obtain viral particles. The lentiviral preparation was then used to infect NSCLC cells in the presence of 8 µg/mL polybrene (Merck Millipore, Darmstadt, Germany). Following 24 h of infection, the cells were further cultured in the presence of puromycin (Merck Millipore, Darmstadt, Germany) for 48 h to select for successfully transduced cells.

Isolation of peripheral blood mononuclear cells (PBMCs) and activation of T cells

PBMCs were obtained from the buffy coat of healthy donors in accordance with guidelines and regulations approved by the Institutional Review Board of Thai Red Cross Society (IRB approval No. 7/2566). To isolate PBMCs, Ficoll-Paque PLUS density gradient media (Cytiva Life Sciences, Marlborough, MA, USA) was used, followed by centrifugation based on density. The isolated PBMCs were then seeded in a 12-well plate containing AIM-V cell culture medium (Gibco) and incubated for 2 h at 37 °C to allow for monocyte cell adhesion. The resulting cell suspension consisted of non-adherent T cells, which were subsequently cultured in AIM-V cell culture medium (Gibco). For T cell activation, T cells were stimulated with Ultra-LEAF Purified anti-human CD3 and CD28 antibodies (BioLegend, San Diego, CA, USA) for 72 h.

Necroptosis induction, co-culture of NSCLC cells and T cells, and cell death detection by Annexin V/PI staining

To induce necroptosis, cells were exposed to a combination of TNF-α (10 ng/mL), Smac mimetic SM-164 (10 nM), and zVAD-fmk (20 µM) for 24 h. Cell death was assessed through Annexin V-FITC and PI staining, followed by flow cytometry analysis. Briefly, cells were washed and then resuspended in Annexin V binding buffer containing recombinant Annexin V-FITC (ImmunoTools, Friesoythe, Germany) and PI (Invitrogen, Carlsbad, CA, USA). The stained cells were analyzed using a BD Accuri™ C6 flow cytometer (BD Biosciences, Franklin Lakes, NJ, USA). Each sample generated data from a total of ten thousand events, and the results were analyzed using BD Accuri™ C6 Software. For co-culture experiments, PBMC-derived T cells were pre-labeled with CellBrite® Red Cytoplasmic Membrane Dyes (Biotium, Fremont, CA, USA) before co-culturing with NSCLC cells. Subsequently, Annexin V-FITC and PI staining was performed on all cells. The cell death of NSCLC cells due to T-cell killing was evaluated by the exclusion of CellBrite® Red-positive T cells.

Statistical analysis

SPSS software was used to analyze all statistical analysis data. For survival analysis, 125 NSCLC patients were divided into low- and high- expression based on the median of modified H-score. Kaplan–Meier and log-rank test were used to compare patient survival between two groups using R's "*survminer*" package. Multivariate analysis with cox-regression of overall survival (OS) was performed to identify independent prognostic factors in NSCLC. The clinical factors were divided into two groups using median as a cutoff. The correlation between two continuous variables was analyzed using Pearson's correlation method. Fisher's exact test was used to analyze the relationship between two group variables. Independent sample t-test method was performed to compare significantly different between the means of two independent groups. Statistically significant was defined when P-value < 0.05 and * was used as a symbol.

Results

High RIPK3 expression was associated with a longer overall survival (OS) of NSCLC patients

In order to explore the clinical significance of RIPK3 and MLKL in NSCLC tissues, IHC was performed to examine the protein expression levels of RIPK3 and MLKL in lung tumors compared to paired adjacent non pathological lung tissues from 125 NSCLC cases. RIPK3 was mainly immunolocalized in the cytoplasm of tumor cells and normal pneumocytes and significantly higher in tumor area than in epithelial cells in adjacent lung tissues (*P*-value = 1.85E-0.09) (Fig. S2A). MLKL was mainly immunolocalized in the cytoplasm of tumor cells and normal pneumocytes. Of particular interest, the localization of MLKL in nucleus or nuclear and cytoplasmic localization in tumor cells were also detected in some cases of NSCLC (Fig. S2B and C). As in RIPK3, MLKL status was significantly higher in tumor than adjacent lung tissues (*P*-value = 6.85E-0.12) (Fig. S2D). In addition, the status of a specific marker of necroptosis activation, pMLKL was also evaluated in this study. The number of pMLKL-positive and pMLKL-negative cases was 27 and 98 cases, respectively (Fig. S3A). Aggregation of pMLKL protein was found in some parts of plasma membrane. In addition, pMLKL-positive cells harbored marked nuclear atypia and shrinkage of nucleus consistent with the morphological features undergoing the process of necroptosis. It is true that necrotic appearance naturally occurs in non-necroptotic tumor cells, but the pMLKL-positive area demonstrated more marked nuclear atypia than others, implying that this phenomenon could occur as a result of necroptosis activation (Fig. S3B). Therefore, in order to further explore the clinical significance of RIPK3, MLKL and pMLKL in NSCLC patients, RIPK3 and MLKL status was tentatively classified into low and high groups using the median of modified H-score as a cut-off, while pMLKL into positive and negative groups (Fig. 1A-C). Interestingly, high RIPK3 status in tumor cells was significantly associated with a longer OS in NSCLC and a LUAD subtype (NSCLC: *P*-value = 0.009, LUAD: *P*-value = 0.032) (Fig. 1D). There were no statistically significant correlations between MLKL or pMLKL and OS in all subtypes of NSCLC (MLKL, NSCLC: *P*-value = 0.267, LUAD: *P*-value = 0.110; pMLKL, NSCLC: *P*-value = 0.151, LUAD: *P*-value = 0.397) (Fig. 1E-F and S4A-C). The correlation among the key necroptotic proteins (RIPK3, MLKL and pMLKL) were further analyzed. There was a significant positive correlation between RIPK3 and MLKL (NSCLC, r = 0.441, *P*-value = 2.71E-0.07; LUAD, r = 0.516, *P*-value = 8.86E-0.08; Fig. 2A), while pMLKL positively correlated with RIPK3 (NSCLC, *P*-value = 4.48E-0.05; LUAD, *P*-value = 1.37E-0.05; Fig. 2B) and MLKL (NSCLC, *P*-value = 2.44E-0.07; LUAD, *P*-value = 2.87E-0.05; Fig. 2C). Therefore, these results all indicated the clinical significance of necroptosis and key necroptotic proteins and suggest RIPK3 as a key necroptotic factor-associated with OS in NSCLC patients.

RIPK3 as an independent prognostic factor in NSCLC patients

In order to further explore whether RIPK3 could serve as an independent prognostic factor for NSCLC patients, univariate and multivariate analysis of OS were performed. When analyzed by using univariate analysis, CD163 + M2 macrophages and RIPK3 were significantly associated with OS (CD163: *P*-value = 0.046, HR = 0.376, RIPK3: *P*-value = 0.015, HR = 0.282) (Table 1). Of particular interest, in multivariate analysis, only RIPK3 status turned out as an independent prognostic factor for OS, suggesting that RIPK3 is a favorable prognostic factor in NSCLC patients (*P*-value = 0.020, HR = 0.296) (Table 1).

The correlation between key necroptotic factors with tumor-infiltrating immune cells (TIICs) in NSCLC

Tumor cells undergoing necroptosis could possibly release inflammatory cytokines/chemokines leading to forming an inflammatory TME, subsequently resulting in enhancement of the infiltration of TIICs. We therefore sought to analyze the correlation between the status of key necroptotic factors and CD8 + T cells, a major anti-tumor immune cells, CD163 + M2 macrophages and Forkhead box protein P3 (FOXp3 +) regulatory T (Treg) cells (FOXp3 + T cells), two major immunosuppressive cells. RIPK3 immunoreactivity was significantly negatively correlated with CD8 + T cells in NSCLC (r = -0.177, *P*-value = 0.049) and LUAD (r = -0.212, *P*-value = 0.039) (Fig. 3A) and positively correlated with CD163 + M2 macrophages in LUAD (r = 0.243, *P*-value = 0.017) (Fig. 3B), while there were no correlations with FOXp3 + T cells (Fig. 3C). MLKL immunoreactivity was not correlated with CD8 + T cells (Fig. 4A), however it was significantly positively correlated with CD163 + M2 macrophages in NSCLC (r = 0.227, *P*-value = 0.011) and LUAD (r = 0.332, *P*-value = 0.001) (Fig. 4B) and FOXp3 + T cells in LUAD (r = 0.174, *P*-value = 0.092) (Fig. 4C). In addition, pMLKL was also significantly positively correlated with CD163 + M2 macrophages in NSCLC (*P*-value = 0.045) and LUAD (*P*-value = 0.010) (Fig. 5B), but not with CD8 + T cells (Fig. 5A) or FOXp3 + T cells (Fig. 5C). These results above all indicated the association between necroptosis and the recruitment of CD163 + M2 macrophages with suppression of the infiltration of CD8 + T cells suggesting the potential correlation between necroptosis and immunosuppressive TME in NSCLC patients.

The association between key necroptotic factors and ICI responsiveness in NSCLC

Infiltration of T cells has been known as one of important factors for ICI-mediated antitumor immune responses. Results of our present study demonstrated the association between necroptosis and key necroptotic proteins in conjunction with the infiltration of TIICs in NSCLC. We therefore hypothesized that necroptosis of tumor cells could alter the infiltration of immune cells in TME and subsequently influence the clinical response to ICI therapy in individual patients. PD-L1 status in tumor cells is currently an FDA-approved predictive biomarker used for the patient selection for ICI therapy in NSCLC. Therefore, we analyzed the correlation between the status of PD-L1 and RIPK3, MLKL or pMLKL in 23 cases of NSCLC who had received ICI therapy. There was no significant correlation between PD-L1 and RIPK3, MLKL or pMLKL in NSCLC patients received ICI therapy (Fig. S5). All 21 cases expressed relatively abundant PD-L1 immunoreactivity but only 12 cases responded to ICI therapy and there was no significant correlation between PD-L1 status and ICI response (Table 2). Therefore, we examined the association between key necroptotic factors and therapeutic efficacy of ICI therapy. Clinicopathological

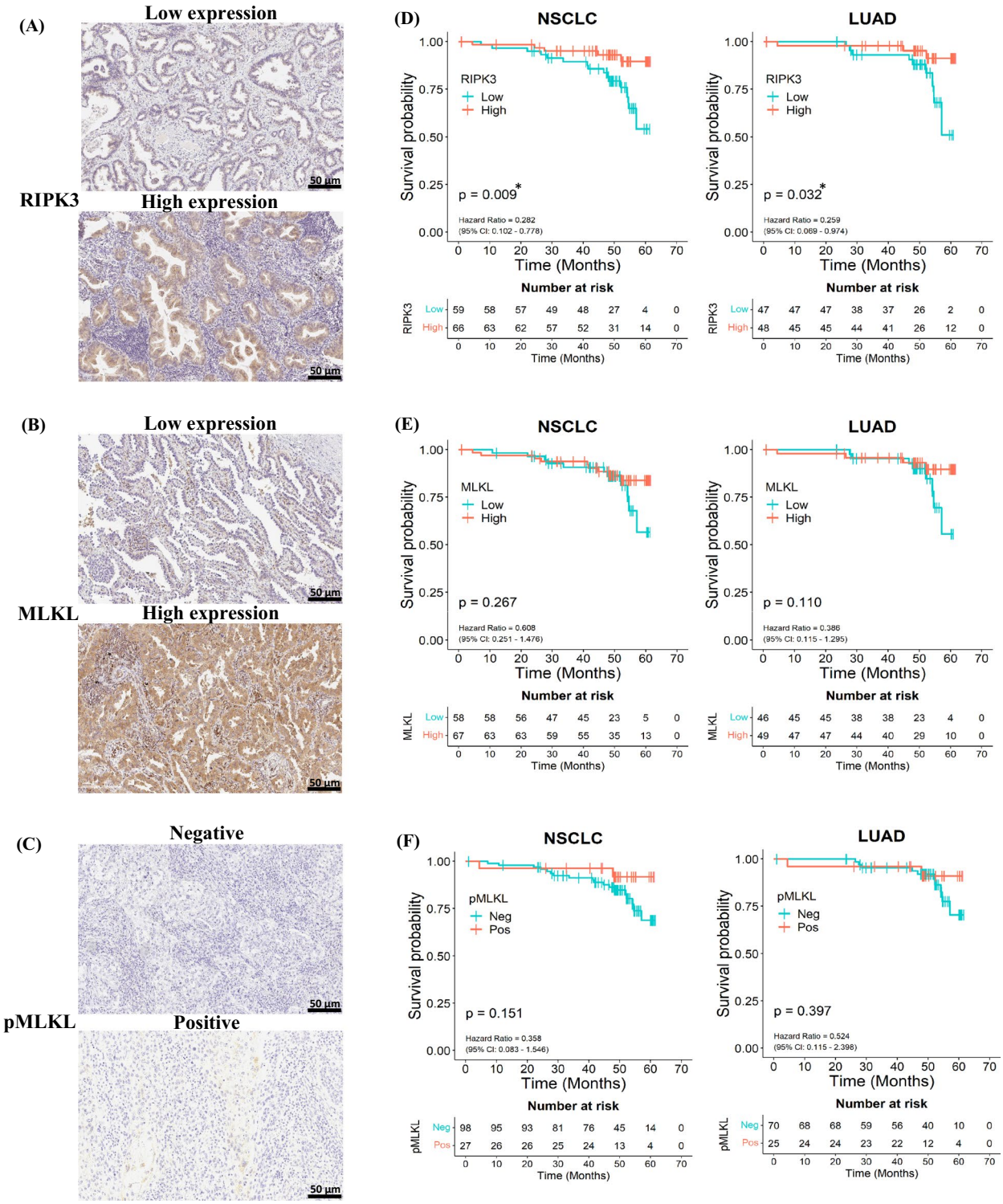

Fig. 1. The associations between the expression of key necroptotic proteins with survival rates in NSCLC patients: Representative images of low and high expression group of (**A**) RIPK3 (**B**) MLKL (**C**) pMLKL. Kaplan–Meier overall (OS) curves divided by the median of modified H-score of (**D**) RIPK3 (**E**) MLKL (**F**) pMLKL in NSCLC, LUAD, respectively. **P*-value < 0.05. *95% CI* 95% Confidence Interval, *HR* hazard ratio, *NSCLC* non-small cell lung, *LUAD* lung adenocarcinoma, *LUSC* lung squamous cell carcinoma.

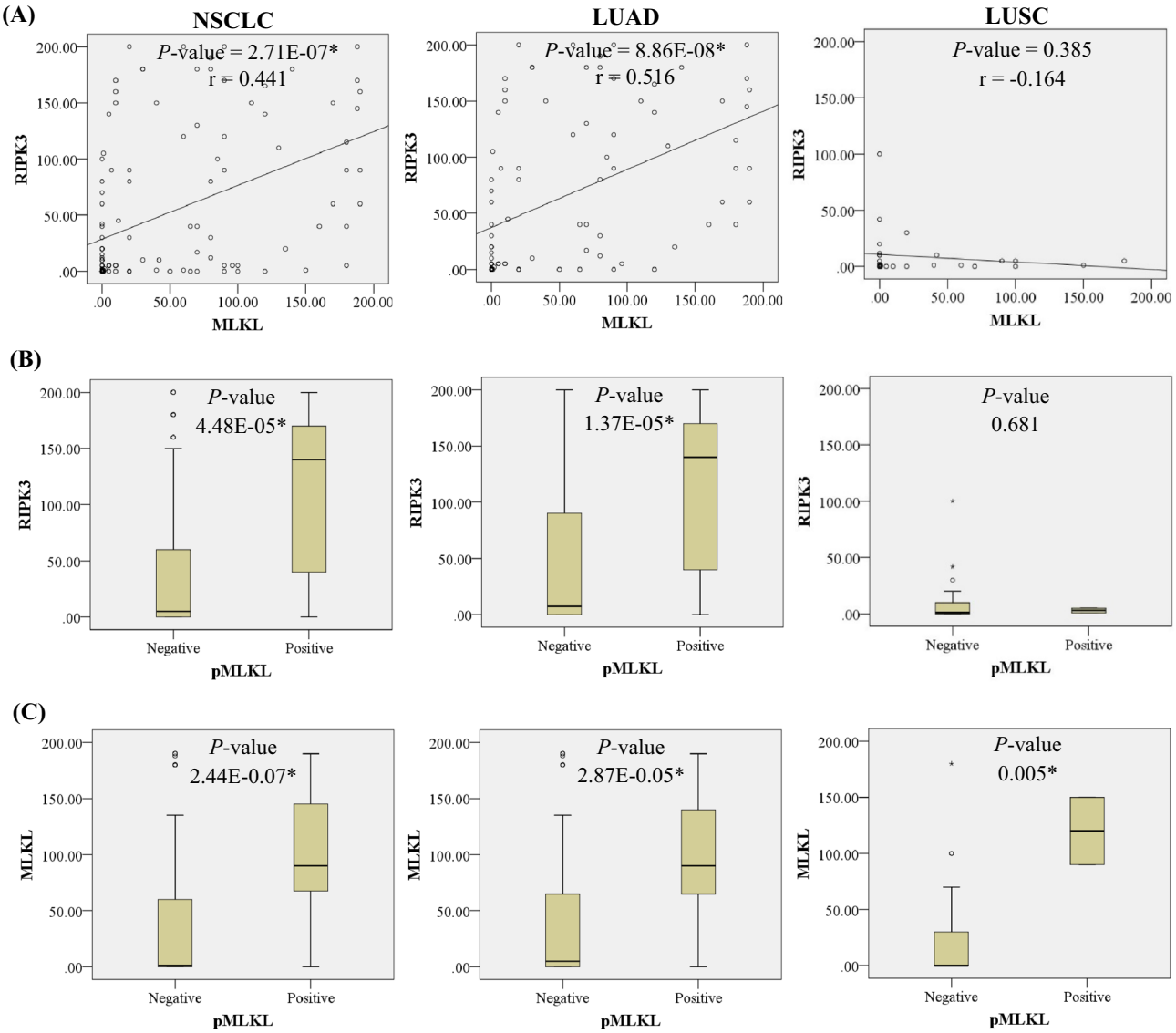

Fig. 2. The correlation among key necroptotic proteins in NSCLC: (**A**) Scatter plot showing the association between RIPK3 and MLKL. Box plots representing the distributions of RIPK3 (**B**) and MLKL (**C**) in a specific marker of necroptosis activation (pMLKL) group. **P*-value < 0.05. *NSCLC* non-small cell lung, *LUAD* lung adenocarcinoma, *LUSC* lung squamous cell carcinoma.

factors of all 23 cases were summarized in Table S2. Among key necroptotic markers examined in this study, high RIPK3 status tended to be associated with clinical therapeutic resistance to ICI therapy, particularly in LUAD subtype (*P*-value = 0.057) (Table 3). This result suggests that RIPK3 could be a new indicator associated with ICI response.

Validation of the correlation between key necroptotic factors and ICI therapeutic response using TISIDB bioinformatic tool

To further validate the association between key necroptotic factors and ICI therapeutic response, we also validated our findings in online public database. Immunotherapy mode in TISIDB bioinformatic tools analyzed the genomic profiles of pre-treatment tumor biopsy from patients treated with immunotherapy. Similar to NSCLC tissues, high RIPK3 expression was significantly correlated with poor outcomes in urothelial cancer patients treated with anti-PD-L1 (atezolizumab) (*P*-value = 0.00967) (Fig. 6A). In addition, the non-responders in melanoma treated with anti-PD-1 (pembrolizumab and nivolumab) also showed higher MLKL expression than a response group (*P-value* = 0.0196) (Fig. 6B). These results further supported our findings suggesting that high expression of key necroptotic factors might contribute to the poor response of ICI therapy.

The responsiveness of T cells to ICIs in NSCLC cells expressing RIPK3

To further substantiate our clinical and bioinformatic findings, we incorporated in vitro experiments to assess the impact of RIPK3 on the responsiveness to ICIs in NSCLC cells. The expression levels of RIPK3 and PD-L1

Factors	Univariate				Multivariate			
	95% CI		HR	*P*-value	95% CI		HR	*P*-value
Gender	0.762	6.825	2.281	0.140				
Age (MED = 69 years)	0.526	3.069	1.270	0.595				
Histological type	0.981	6.417	2.510	0.055				
EGFR mutation	0.270	2.254	0.781	0.647				
KRAS mutation	0.355	7.620	1.645	0.524				
Smoking status	0.611	5.582	1.846	0.277				
Tumor size (MED = 26 mm)	0.614	3.707	1.509	0.369				
Pathological stage	0.514	3.895	1.415	0.502				
PD-L1 (MED = 120)	0.308	1.793	0.743	0.508				
CD8 + TILs	0.494	2.881	1.194	0.694				
CD163 + M2 macrophages	0.144	0.984	0.376	0.046*	0.153	1.059	0.403	0.065
FOXP3 + TILs	0.217	1.301	0.532	0.167				
RIPK3 (MED = 10)	0.102	0.778	0.282	0.015*	0.107	0.823	0.296	0.020*
MLKL (MED = 10)	0.251	1.476	0.608	0.272				
pMLKL	0.083	1.546	0.358	0.169				

Table 1. Univariate and multivariate Cox proportional hazard analysis overall-survival (OS) of NSCLC patients. **P*-value < 0.05. *95% CI* 95% Confidence Interval, *EGFR* Epidermal growth factor receptor, *HR* hazard ratio, *KRAS* Kirsten rat sarcoma viral oncogene homolog.

in NSCLC cell lines, including A549, HCC827, and H1975 were examined. Our results revealed that none of these cell lines expressed RIPK3, and A549 also did not express PD-L1 (Fig. 7A). Subsequently, we transduced H1975 cells with lentiviral particles to induce the expression of RIPK3 (Fig. 7B). The functionality of RIPK3 as a key necroptotic molecule in these cells was validated. H1975 cells expressing RIPK3 exhibited significantly increased sensitivity to necroptosis compared to NSCLC cells with a control vector (*P*-value = 0.001) (Fig. 7C). To investigate the role of RIPK3 in NSCLC cells on T cells responsiveness to ICIs, we conducted co-culture experiments with peripheral blood mononuclear cell (PBMC)-derived T cells, which were pre-activated with CD3/CD28, as depicted in Fig. 7D. The results demonstrated that both vector control and RIPK3-overexpressing H1975 cells, when co-cultured with activated T cells, underwent cell death to a similar extent. Additionally, when treated with pembrolizumab, a PD-1 monoclonal antibody, H1975 cells with vector control exhibited increased responsiveness to T cell-mediated killing compared to those treated with an isotype control (*P*-value = 0.037). Interestingly, RIPK3-overexpressing H1975 cells showed significantly reduced responsiveness to T cell-mediated killing in the presence of pembrolizumab (*P*-value = 0.012). These findings suggest that RIPK3 may play a role in modulating responsiveness to ICIs (Fig. 7E).

Discussion

In this study, we identified RIPK3 as an independent favorable prognostic factor in NSCLC patients. This is the first study to demonstrate a significantly positive correlation between the status of key necroptotic proteins (i.e., RIPK3, MLKL, pMLKL) and CD163 + M2 macrophages, while an inverse correlation was detected between key necroptotic proteins and CD8 + T cells. These results all suggest crosstalk or interplay between necroptosis of tumor cells and an immunosuppressive tumor microenvironment (TME) in NSCLC patients. Additionally, while it is true that ICI therapeutic response might not be directly linked to PD-L1 status of tumor cells, we did demonstrate that key necroptotic proteins, particularly RIPK3, tended to be associated with therapeutic resistance to ICI therapy in NSCLC patients who had received ICI therapy. Furthermore, we showed that NSCLC cells-expressing RIPK3 suppressed T cell response to ICI therapy in vitro. This result suggests that RIPK3 could be a new indicator associated with ICI response. We propose that necroptosis could induce an immunosuppressive microenvironment, resulting in a poor response to ICI therapy in NSCLC, but it awaits further investigation for clarification. (Fig. 8).

Several studies have reported the association between key necroptotic proteins and survival of the patients in various human malignancies[26–30,32,42,43]. However, there has been some discrepancies in terms of whether key necroptotic proteins were associated with good or poor prognoses which could be depended on the types and stages of cancers and cellular context in TME. There are only a few studies reporting the clinical relevance of necroptosis in lung cancer patients. The status of RIPK1, RIPK3 and MLKL was all significantly lower in NSCLC tissues than in adjacent lung tissues and their low expression status was also significantly associated with a worse disease free survival (DFS)[25]. In addition, low RIPK3 status was also associated with a shorter overall survival (OS) in lung cancer patients with a squamous cell carcinoma subtype of stage I NSCLC[44]. In consistent with the previous studied, we demonstrated that the lower status of RIPK3 was significantly associated with unfavorable prognosis in NSCLC patients. In addition, this is the first study to explore the association of MLKL and a specific marker of necroptosis activation, pMLKL in NSCLC patients. There were no significant associations between MLKL or pMLKL and OS of NSCLC patients, but further correlation analysis revealed the positive correlation among key necroptotic factors (i.e., RIPK3, MLKL, pMLKL). Therefore, these results all suggest that lung cancer

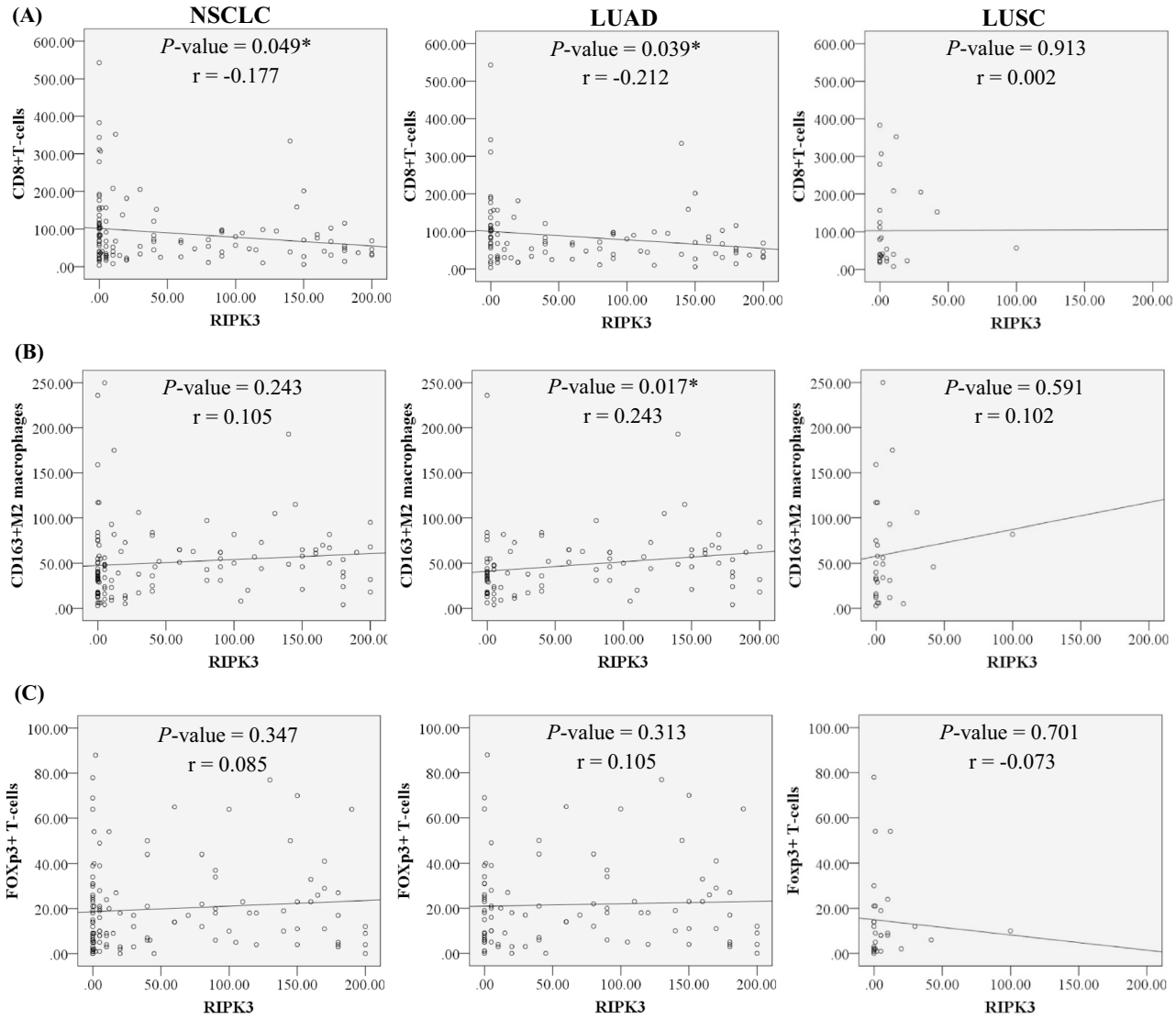

Fig. 3. The correlation between RIPK3 expression with inflammatory/immune cells infiltration in NSCLC tissues: Scatter plots showing the correlation between RIPK3 and CD8 + T-cells (**A**), CD163 + M2 macrophages (**B**), FOXp3 + T-cells (**C**). **P*-value < 0.05. *NSCLC* non-small cell lung, *LUAD* lung adenocarcinoma, *LUSC* lung squamous cell carcinoma.

patients with high RIPK3 expression were more likely to activate necroptosis signaling. In addition, among key necroptotic factors, RIPK3 is considered as an independent favorable prognostic marker in patients with NSCLC. The results of these studies all suggest that the correlation between the abundance of RIPK3 and a good prognosis could occur as a result of increased necroptosis signaling, leading to increased tumor killing in these patients. Several growing evidence have also reported that some anticancer drugs, chemotherapy and radiotherapy can induce acute massive necroptosis[33]. Therefore, the patients with high RIPK3 expression are more likely to benefit from regular treatments, resulting in a good prognosis. We attempted to analyze the correlation of RIPK3 and OS in patients who received adjuvant chemotherapy, however only 32 out of 125 patients received adjuvant chemotherapy, while 52 patients did not receive adjuvant chemotherapy and data of 41 patients was missing (Table S3A–C). In NSCLC patients who received adjuvant chemotherapy, the mean survival of patients with high and low RIPK3 was 60.82 ± 0.76 months and 57.14 ± 2.20 months, respectively, however it did not reach statistically significant (*P*-value = 0.394) (Table S3D), probably due to low sample size. This is consistent with a study in lung adenocarcinoma in which patients who underwent cisplatin-based adjuvant chemotherapy after tumor resection with high RIPK3 expression have a prolonged DFS[45]. In addition, a study in NSCLC further supports the previous findings that patients with high expression of RIPK3 was associated with improved progression-free survival following ablative hypofractionated radiation therapy[46].

Accumulating evidence has reported the link between necroptosis of tumor cells and immune TME, although the roles of necroptosis in tumor immunity remain unestablished[32,33,37,38,47]. Mild degree of spontaneous chronic necroptosis of tumor cells which could be triggered under metabolic stress in TME was reported to modulate inflammatory responses creating immunosuppressive microenvironment. However, to the best of our knowledge,

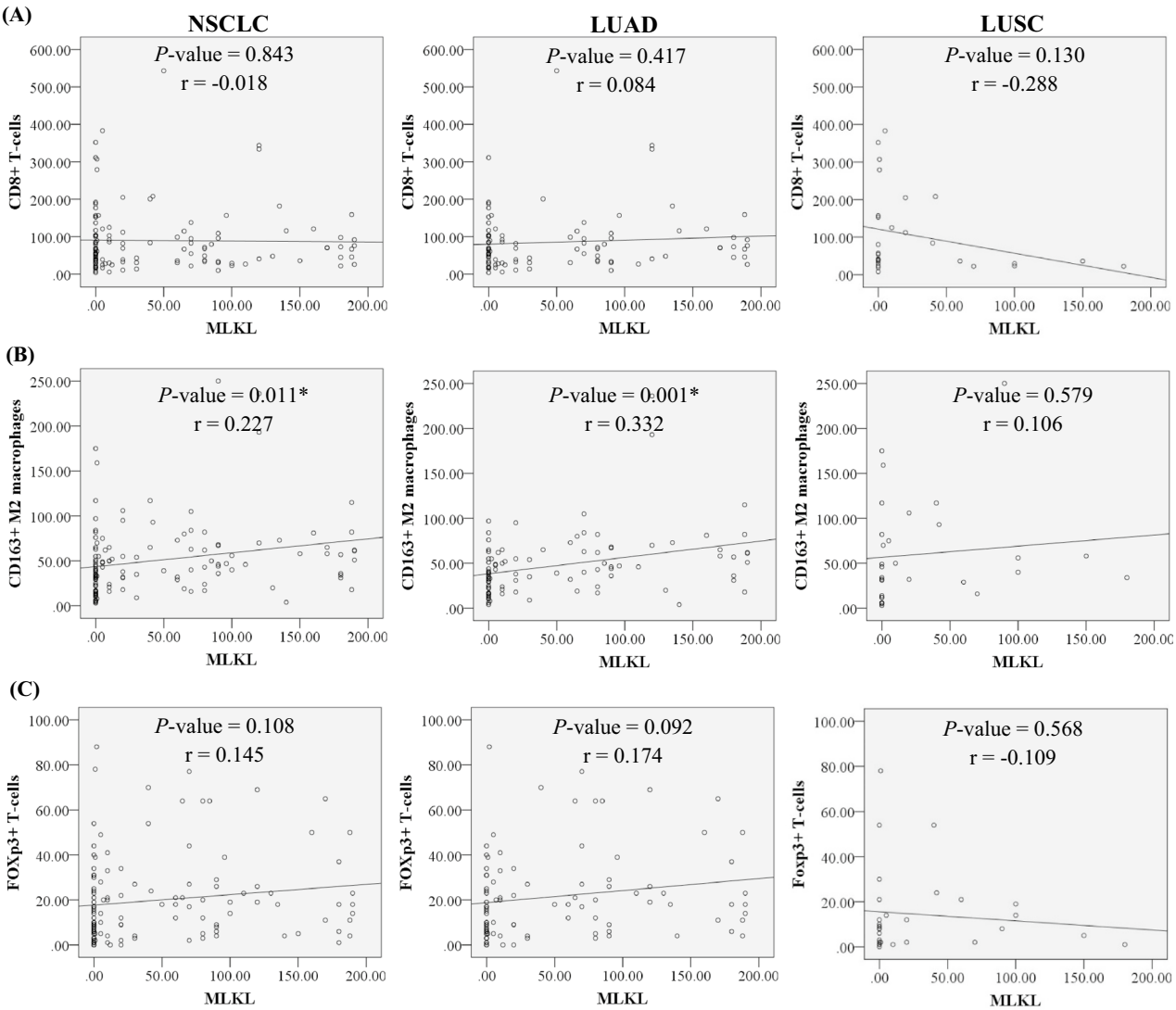

Fig. 4. The correlation between MLKL expression with inflammatory/immune cells infiltration in NSCLC tissues: Scatter plots showing the correlation between MLKL and CD8 + T-cells (**A**), CD163 + M2 macrophages (**B**), FOXp3 + T-cells (**C**). **P*-value < 0.05. *NSCLC* non-small cell lung, *LUAD* lung adenocarcinoma, *LUSC* lung squamous cell carcinoma.

the interplay or crosstalk between key necroptotic factors (RIPK3, MLKL and pMLKL) and TIICs in NSCLC TME has not been reported in the literature. Of particular interest, all three key necroptotic factors were significantly positively correlated with CD163 + M2 macrophages infiltration in NSCLC and a LUAD subtypes, although the correlation did not reach statistical significance in LUSC subtype, most likely due to a small sample size. In addition, MLKL status was significantly positively correlated with FOXp3 + T cells in the LUAD subtype, while RIPK3 negatively correlated with CD8 + T cells in NSCLC and the LUAD subtype. Altogether, significantly positive correlation was demonstrated between the status of key necroptotic proteins and two major immunosuppressive cells (CD163 + M2 macrophages or Foxp3 + T cells), while a negative one between key necroptotic proteins and a major anti-tumor immune cell, CD8 + T cells detected suggesting the interplay between necroptosis of tumor cells and an immunosuppressive TME in NSCLC. These results were also consistent with those of previous studies in breast cancer and PDAC[37,47]. In PDAC experimental mouse model, Seifert *et al.* demonstrated that RIPK3 created immunosuppressive TME by enhancing CD163 + M2 macrophages and MDSCs through releasing CXCL1 and SAP130 chemokines[37]. In accordance with this study of PDAC, a recent study in breast cancer using a genetic modified MMTV-PyMT model and an orthotopic transplantation MVT-1 model have demonstrated that tumor necroptosis promoted metastasis through inhibiting the anti-tumor activity of CD8 + T cells[47]. Similarly, a study in melanoma also demonstrated that necroptosis of tumor cells released a relatively high level of potassium leading to the suppression of T cell effector function and subsequently resulting in inhibition of anti-tumor immunity[48]. Results of our present study therefore provided the first evidence in NSCLC showing the association between necroptosis of tumor cells and immunosuppressive TME but further studies using a larger NSCLC cohort and in vitro and in vivo are warranted to explore the role of necroptosis and immune TME.

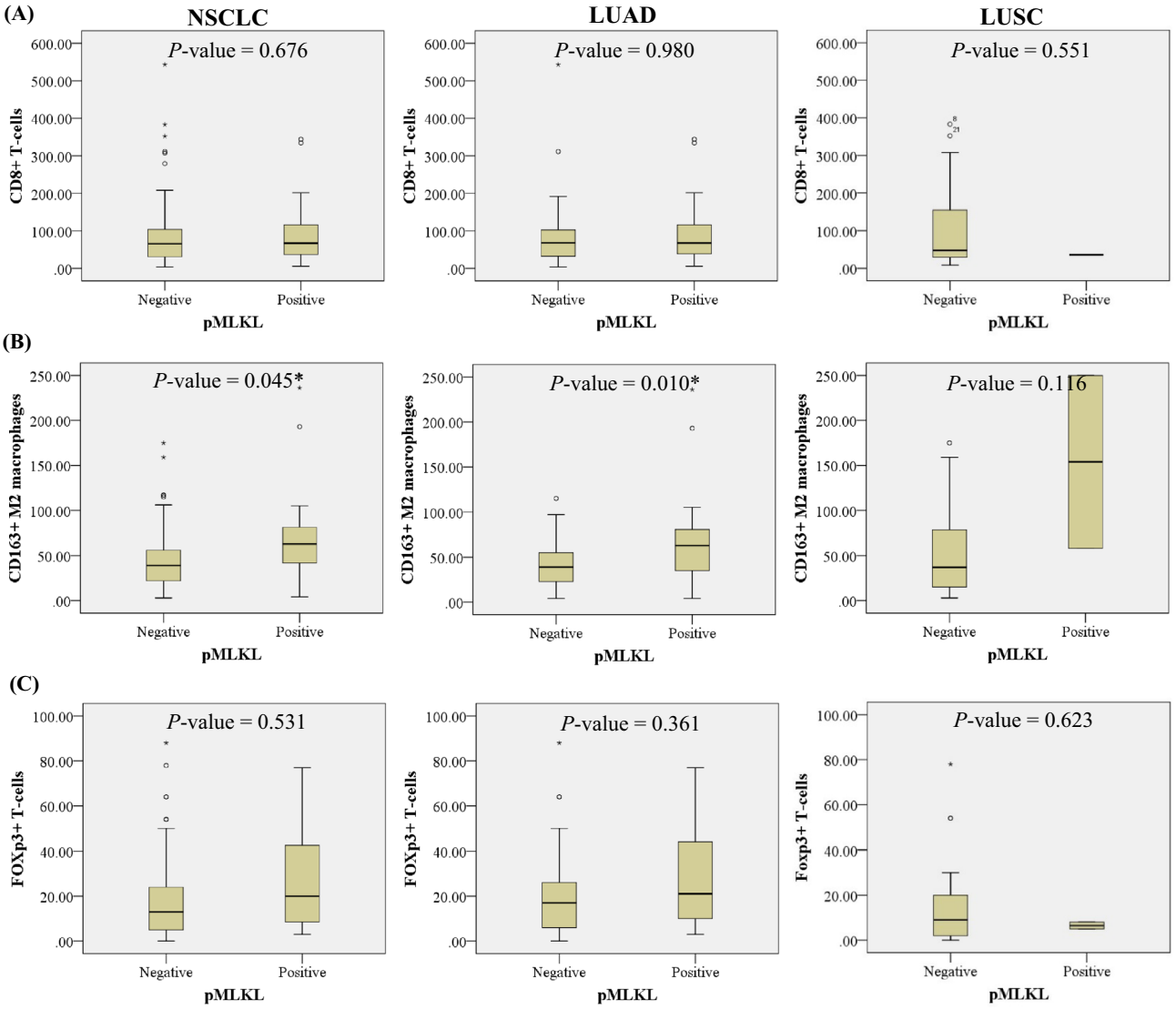

Fig. 5. The distributions of inflammatory/immune cells infiltration in a specific marker of necroptosis activation (pMLKL) negative and positive groups of NSCLC tissues: Box plots showing the distributions of tumor-infiltrating CD8 + T-cells **(A)**, CD163 + M2 macrophages **(B)**, and FOXp3 + T-cells **(C)** in a specific marker of necroptosis activation (pMLKL) negative and positive groups. **P*-value < 0.05. *NSCLC* non-small cell lung, *LUAD* lung adenocarcinoma, *LUSC* lung squamous cell carcinoma.

Factor	Total (n = 21)				LUAD (n = 16)				LUSC (n = 5)			
	Number of patients	PD-L1		*P*	Number of patients	PD-L1		*P*	Number of patients	PD-L1		*P*
		Low	High			Low	High			Low	High	
Therapeutic efficacy of ICI												
Non-responder (SD + PD)	9	7	2	0.367	9	7	2	0.126	0	0	0	N/A
Responder (CR + PR)	12	6	6		7	2	5		5	4	1	

Table 2. The correlation between immunoreactivity of PD-L1 expression on tumor cells and therapeutic efficacy of ICI therapy in NSCLC.

The status of intratumoral immune TME is one of the important factors contributing to ICI response[7,8]. Since our results have suggested that necroptosis and key necroptotic factors might be associated with immunosuppressive TME in NSCLC, we therefore hypothesized that necroptosis could contribute to a low therapeutic response to ICI therapy through its possible role in modulating immune TME in NSCLC. Therefore, we examined the association between key necroptotic factors (RIPK3, MLKL, pMLKL) and therapeutic efficacy of ICI therapy

Factor	Total (n = 23)				LUAD (n = 17)				LUSC (n = 6)			
	Number of patients	RIPK3		*P*	Number of patients	RIPK3		*P*	Number of patients	RIPK3		*P*
		Low	High			Low	High			Low	High	
Therapeutic efficacy of ICI												
A												
Non-responder (SD + PD)	9	2	7	0.197	9	2	7	0.057	0	0	0	N/A
Responder (CR + PR)	14	8	6		8	6	2		6	3	3	
B												
Non-responder (SD + PD)	9	4	5	0.799	9	4	5	0.824	0	0	0	N/A
Responder (CR + PR)	14	7	7		8	4	4		6	3	3	
C												
Non-responder (SD + PD)	9	5	4	0.657	9	5	4	0.824	0	0	0	N/A
Responder (CR + PR)	14	10	4		8	4	4		6	6	0	

Table 3. The correlation between immunoreactivity of RIPK3, MLKL and a specific marker of necroptosis activation (pMLKL) and therapeutic efficacy of ICI therapy in NSCLC. *CR* complete response, *LUAD* lung adenocarcinoma, *LUSC* lung squamous cell carcinoma, *MLKL* mixed lineage kinase domain-like, *NSCLC* non-small cell lung cancer, *PD* progressive disease, *pMLKL* phosphorylated mixed lineage kinase domain-like, *PR* partial response, *RIPK3* receptor-interacting protein kinase 3, *SD* stable disease.

in 23 NSCLC patients who received ICI therapy. There were no statistically significant correlations among key necroptotic factors and PD-L1, the U.S FDA-approved biomarker for predicting ICI response in NSCLC, on tumor cells. However, high RIPK3 status tended to be correlated with resistance to ICI therapy in the LUAD subtype (*P*-value = 0.057). In addition, to further validate our results in NSCLC, we also used TISIDB bioinformatic tools to analyze the genomic profiles of pre-treatment tumor biopsies from patients treated with immunotherapy. Like NSCLC tissues, high RIPK3 expression was significantly correlated with poor outcomes in urothelial cancer patients treated with anti-PD-L1 (atezolizumab), while in melanoma treated with anti-PD-1 (pembrolizumab and nivolumab), the non-responders expressed a higher level of MLKL than the response group. Therefore, our results suggest that RIPK3 might be a novel biomarker associated with ICI response in NSCLC, particularly lung adenocarcinoma. Although all three necroptotic factors were positively correlated with CD163 + M2 macrophages in NSCLC and LUAD subtypes, only RIPK3 was negatively correlated with CD8 + T cells, which is particularly critical factor for ICI response. This difference may explain why RIPK3 correlates with poor response to ICI therapy specifically in LUAD. Unfortunately, due to NSCLC tissue biopsies obtained from patients receiving ICI therapy are very small in size especially in tumor area, hence there were not enough tissue sections to analyze the association of TIICs and the efficacy of ICI response. Furthermore, due to a small sample size in which only 23 NSCLC patients were included in our study, therefore the predictive significance of RIPK3 on the efficacy of ICI response needs further investigation in a lager NSCLC cohort received ICI therapy.

Cancer immunotherapy has been revolutionizing cancer treatment, particularly by harnessing T cell cytotoxicity. However, studying this phenomenon is challenging due to the complexities of animal models. Numerous studies have made efforts to establish in vitro experimental settings aimed at replicating the tumor microenvironment[49]. Our experimental settings remained consistent with previous studies, which demonstrated that H1975 cells were sensitive to cell death when co-cultured with activated T cells[50,51]. However, it is important to note that the degree of sensitivity to T cell-mediated killing may vary based on factors such as the types of inducers and time courses. Subsequently, HCC827 cells were excluded from the co-culture experiments due to their resistance to T cell killing, even when treated with pembrolizumab. This resistance has been previously observed in HCC827 cells, and our findings are in line with these previous results. Notably, HCC827 cells not only demonstrated resistance to T cell killing but also exhibited inhibitory effects on T cell proliferation and induced apoptosis in T cells[52,53]. The evidence compiled from our primary tissue analysis of NSCLC cohorts, bioinformatics analyses, and in vitro experiments strongly supports the role of RIPK3 in contributing to the responsiveness to immune checkpoint inhibitors. Nevertheless, further investigations into the underlying mechanisms are crucial to provide deeper insights into this phenomenon.

In summary, this is the first study in NSCLC to demonstrate that RIPK3 could serve as an independent favorable prognostic factor and could be a new indicator-associated with ICI response in NSCLC patients. This is also the first study highlighting the strong association between necroptosis and TIICs, particularly CD163 + M2 macrophages in NSCLC. We proposed that necroptosis could induce an immunosuppressive microenvironment, resulting in low response to ICI therapy in NSCLC. (Fig. 8) However, there are some limitations in our present study. Firstly, all NSCLC patients received ICI were treated in conjunction with chemotherapy and the correlation between key necroptotic factors and treatment efficacy could reflect the result of the combination effects of ICI treatment and chemotherapy. Secondly, according to tumor heterogeneity, biopsy specimens might not represent the features of the whole tumor. Lastly, additional large-scale studies should be carried out to validate these findings and to increase statistical power, particularly in NSCLC received ICI therapy.

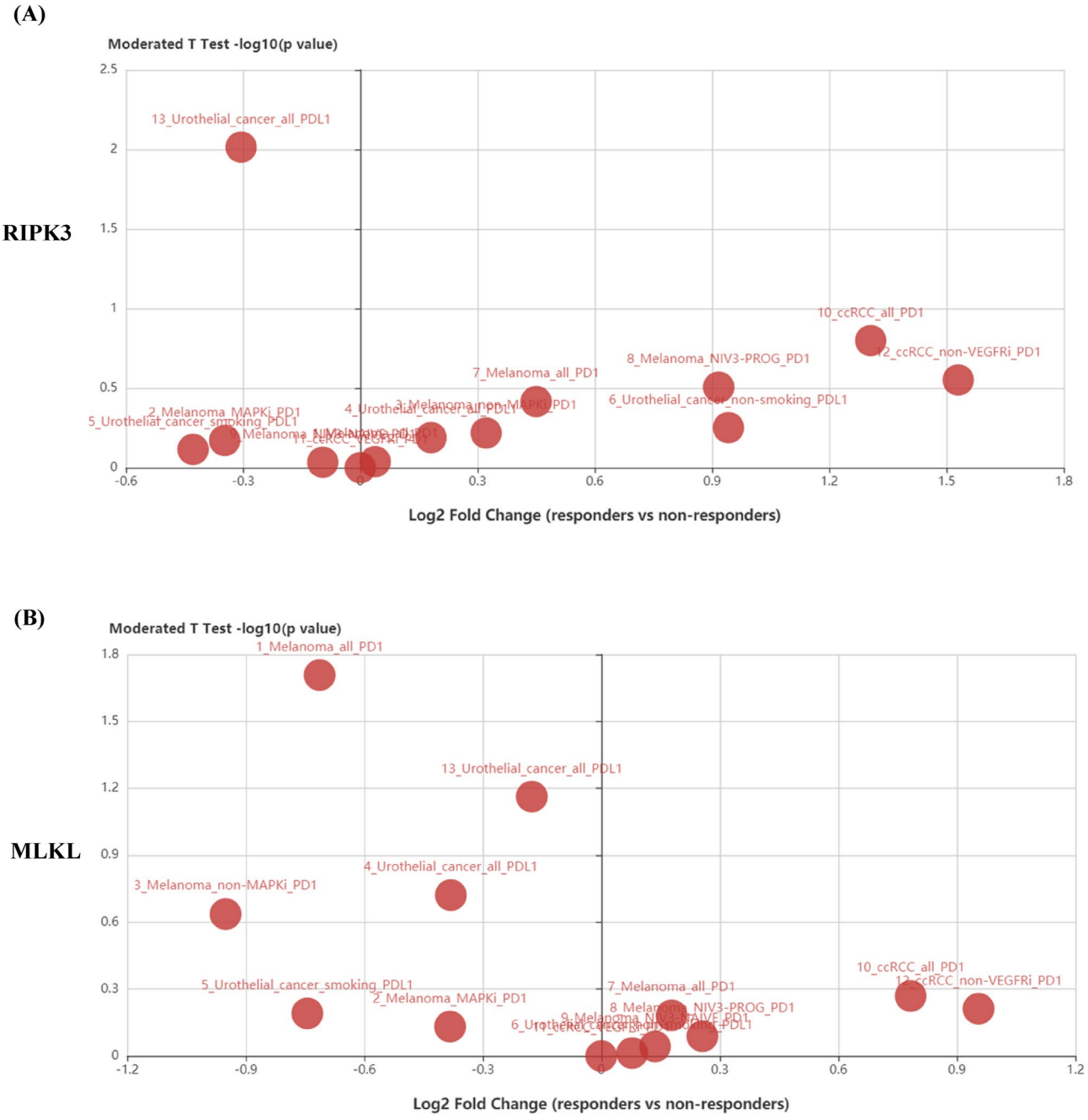

Fig. 6. The differential expression of key necroptotic factors between responders and non-responders to immunotherapy in various data sets analyzed by TISIDB bioinformatic tools: Volcano plot representing the differential expression of (**A**) RIPK3 and (**B**) MLKL between responders and non-responders to immunotherapy in various data sets. Each of red circle in volcano plot represents each of the study, more detail of each study can be obtained by searching PMID. X-axis is – log10(*P*-value) and Y-axis is Log2 (Fold Change). Red arrows present the significantly differential expression of key necroptotic factors between responders and non-responders.

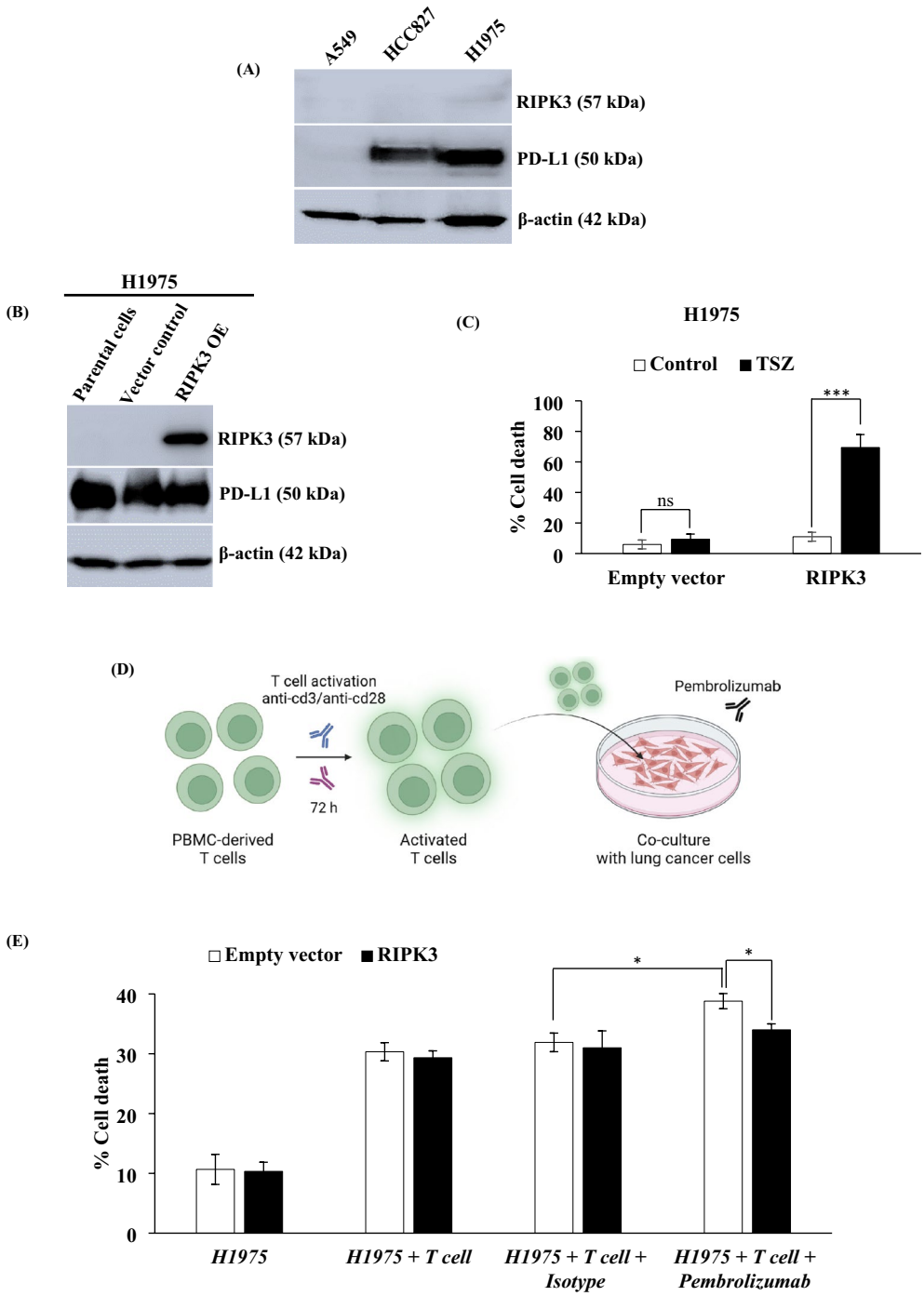

Fig. 7. The impact of RIPK3 expression in NSCLC cells on T-cell responsiveness to immune checkpoint inhibitors: (**A**) Western blot analysis of RIPK3 and PD-L1 expression in NSCLC cells. (**B**) Western blot analysis demonstrating RIPK3 expression in H1975 cell lines following stable lentiviral transduction. (**C**) Bar graph illustrating the percentage of cell death in H1975-expressing RIPK3 cells induced by necroptosis stimuli. (**D**) Illustration displaying the experimental workflow for co-culture between NSCLC cells and PBMC-derived T cells. (**E**) Bar graph representing the percentage of T cell-mediated cell death in H1975-expressing RIPK3 cells in the presence or absence of pembrolizumab. Data represent three independent experiments ± SD. (**P*-value < 0.05, ***P*-value < 0.01, ****P*-value < 0.001); *ns* non-significant.

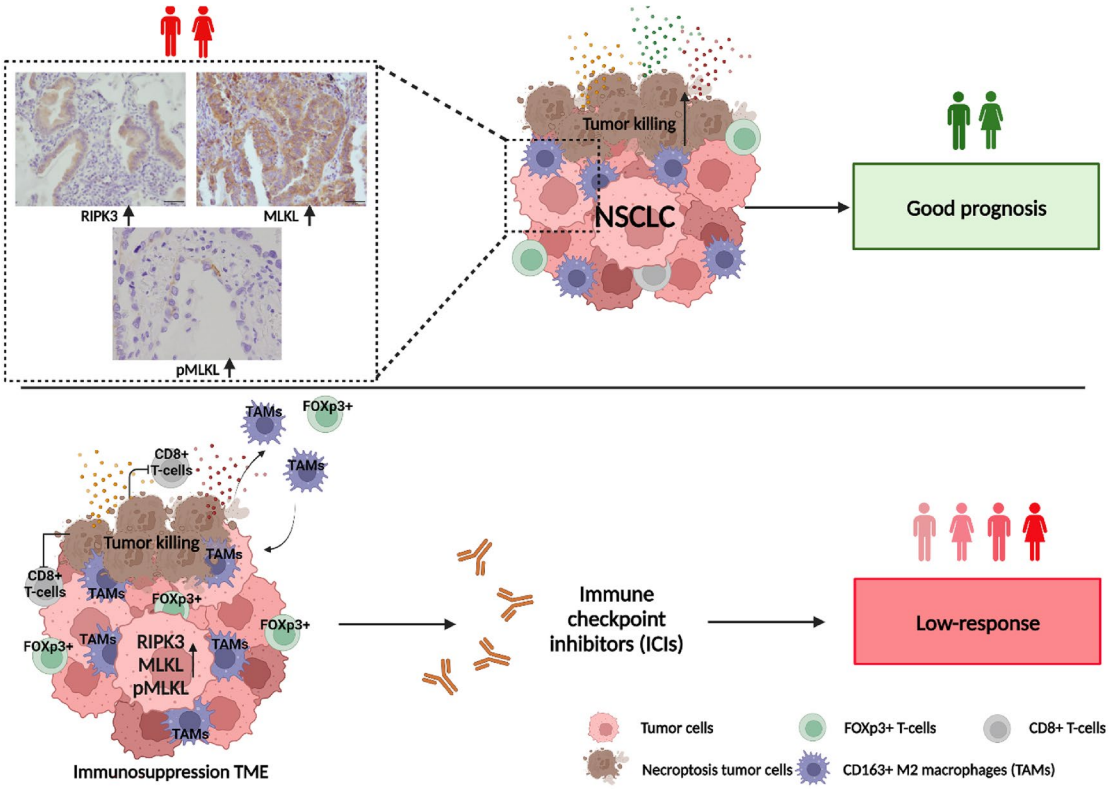

Fig. 8. Graphical conclusions: (**A**) High expression of key necroptotic proteins (RIPK3, MLKL, pMLKL) were positively correlated with survival rates and RIPK3 was an independent prognostic factor for predicting NSCLC prognosis. One possible underlying mechanism for the correlation between high expression of key necroptotic proteins with a good prognosis might be as a result of an increased necroptosis signaling, leading to an increased tumor killing in NSCLC patients. (**B**) Key necroptotic proteins-mediated necroptosis activation might induce an immunosuppressive microenvironment by promoting CD163 + M2 macrophages infiltration, while inhibiting CD8 + T-cells recruitment that might contribute to a low response to ICI therapy in NSCLC patients. *Created with BioRender.com on 1st March 2024.

Data availability

All data are available in the main text or the supplementary materials.

Received: 14 June 2024; Accepted: 9 September 2024
Published online: 16 September 2024

References

1. Sung, H. *et al.* Global cancer statistics 2020: GLOBOCAN estimates of incidence and mortality worldwide for 36 cancers in 185 countries. *CA Cancer J. Clin.* **71**, 209–249 (2021).
2. Duma, N., Santana-Davila, R. & Molina, J. R. Non-small cell lung cancer: Epidemiology, screening, diagnosis, and treatment. *Mayo Clin. Proc.* **94**, 1623–1640 (2019).
3. Siegel, R. L., Miller, K. D., Wagle, N. S. & Jemal, A. Cancer statistics, 2023. *CA Cancer J. Clin.* **73**, 17–48 (2023).
4. Dafni, U., Tsourti, Z., Vervita, K. & Peters, S. Immune checkpoint inhibitors, alone or in combination with chemotherapy, as first-line treatment for advanced non-small cell lung cancer. A systematic review and network meta-analysis. *Lung Cancer* **134**, 127–140 (2019).
5. Herbst, R. S. *et al.* Pembrolizumab versus docetaxel for previously treated, PD-L1-positive, advanced non-small-cell lung cancer (KEYNOTE-010): A randomised controlled trial. *Lancet* **387**, 1540–1550 (2016).
6. Carbognin, L. *et al.* Differential activity of nivolumab, pembrolizumab and MPDL3280A according to the tumor expression of programmed death-ligand-1 (PD-L1): Sensitivity analysis of trials in melanoma, lung and genitourinary cancers. *PLoS One* **10**, e0130142 (2015).
7. Liu, Y. T. & Sun, Z. J. Turning cold tumors into hot tumors by improving T-cell infiltration. *Theranostics* **11**, 5365–5386 (2021).
8. Binnewies, M. *et al.* Understanding the tumor immune microenvironment (TIME) for effective therapy. *Nat. Med.* **24**, 541–550 (2018).
9. Saito, R. *et al.* 11β hydroxysteroid dehydrogenase 1: A new marker for predicting response to immune-checkpoint blockade therapy in non-small-cell lung carcinoma. *Br. J. Cancer* **123**, 61–71 (2020).
10. Fumet, J.-D. *et al.* Prognostic and predictive role of CD8 and PD-L1 determination in lung tumor tissue of patients under anti-PD-1 therapy. *Br. J. Cancer* **119**, 950–960 (2018).
11. Hurkmans, D. P. *et al.* Tumor mutational load, CD8(+) T cells, expression of PD-L1 and HLA class I to guide immunotherapy decisions in NSCLC patients. *Cancer Immunol. Immunother.* **69**, 771–777 (2020).
12. Larroquette, M. *et al.* Spatial transcriptomics of macrophage infiltration in non-small cell lung cancer reveals determinants of sensitivity and resistance to anti-PD1/PD-L1 antibodies. *J. Immuno Ther. Cancer* **10**, e003890 (2022).
13. Gadiyar, V. *et al.* Cell death in the tumor microenvironment: implications for cancer immunotherapy. *Cells* **9**, 2207 (2020).

14. Pitt, J. M., Kroemer, G. & Zitvogel, L. Immunogenic and non-immunogenic cell death in the tumor microenvironment. *Adv. Exp. Med. Biol.* **1036**, 65–79 (2017).
15. Holler, N. *et al.* Fas triggers an alternative, caspase-8-independent cell death pathway using the kinase RIP as effector molecule. *Nat. Immunol.* **1**, 489–495 (2000).
16. Cho, Y. S. *et al.* Phosphorylation-driven assembly of the RIP1-RIP3 complex regulates programmed necrosis and virus-induced inflammation. *Cell* **137**, 1112–1123 (2009).
17. He, S. *et al.* Receptor interacting protein kinase-3 determines cellular necrotic response to TNF-alpha. *Cell* **137**, 1100–1111 (2009).
18. Zhang, D. W. *et al.* RIP3, an energy metabolism regulator that switches TNF-induced cell death from apoptosis to necrosis. *Science* **325**, 332–336 (2009).
19. Sun, L. *et al.* Mixed lineage kinase domain-like protein mediates necrosis signaling downstream of RIP3 kinase. *Cell* **148**, 213–227 (2012).
20. Zhao, J. *et al.* Mixed lineage kinase domain-like is a key receptor interacting protein 3 downstream component of TNF-induced necrosis. *Proc. Natl. Acad. Sci. U. S. A.* **109**, 5322–5327 (2012).
21. Cai, Z. *et al.* Plasma membrane translocation of trimerized MLKL protein is required for TNF-induced necroptosis. *Nat. Cell Biol.* **16**, 55–65 (2014).
22. Dhuriya, Y. K. & Sharma, D. Necroptosis: A regulated inflammatory mode of cell death. *J. Neuroinflamm.* **15**, 199 (2018).
23. Qin, X., Ma, D., Tan, Y. X., Wang, H. Y. & Cai, Z. The role of necroptosis in cancer: A double-edged sword?. *Biochim. Biophys. Acta Rev. Cancer* **1871**, 259–266 (2019).
24. Gong, Y. *et al.* The role of necroptosis in cancer biology and therapy. *Mol. Cancer* **18**, 100 (2019).
25. Park, J. E. *et al.* Expression of key regulatory genes in necroptosis and its effect on the prognosis in non-small cell lung cancer. *J. Cancer* **11**, 5503–5510 (2020).
26. Li, X. *et al.* Association of mixed lineage kinase domain-like protein expression with prognosis in patients with colon cancer. *Technol. Cancer Res. Treat.* **16**, 428–434 (2017).
27. Ertao, Z. *et al.* Prognostic value of mixed lineage kinase domain-like protein expression in the survival of patients with gastric caner. *Tumour Biol.* **37**, 13679–13685 (2016).
28. Feng, X. *et al.* Receptor-interacting protein kinase 3 is a predictor of survival and plays a tumor suppressive role in colorectal cancer. *Neoplasma* **62**, 592–601 (2015).
29. Ruan, J., Mei, L., Zhu, Q., Shi, G. & Wang, H. Mixed lineage kinase domain-like protein is a prognostic biomarker for cervical squamous cell cancer. *Int. J. Clin. Exp. Pathol.* **8**, 15035–15038 (2015).
30. He, L., Peng, K., Liu, Y., Xiong, J. & Zhu, F. F. Low expression of mixed lineage kinase domain-like protein is associated with poor prognosis in ovarian cancer patients. *Onco Targets Ther.* **6**, 1539–1543 (2013).
31. Bozec, D., Iuga, A. C., Roda, G., Dahan, S. & Yeretssian, G. Critical function of the necroptosis adaptor RIPK3 in protecting from intestinal tumorigenesis. *Oncotarget* **7**, 46384–46400 (2016).
32. Nicolè, L., Sanavia, T., Cappellesso, R. et al. Necroptosis-driving genes RIPK1, RIPK3 and MLKL-p are associated with intratumoral CD3(+) and CD8(+) T cell density and predict prognosis in hepatocellular carcinoma. J. Immunother. Cancer 10 (2022).
33. Yan, J., Wan, P., Choksi, S. & Liu, Z. G. Necroptosis and tumor progression. Trends. *Cancer* **8**, 21–27 (2022).
34. Yamauchi, T. *et al.* Necroptosis in esophageal squamous cell carcinoma: An independent prognostic factor and its correlation with tumor-infiltrating lymphocytes. *Cancers* **13**, 4473 (2021).
35. Li, J. *et al.* Necroptosis in head and neck squamous cell carcinoma: characterization of clinicopathological relevance and in vitro cell model. *Cell Death Dis.* **11**, 391 (2020).
36. Dong, Y. *et al.* Upregulated necroptosis-pathway-associated genes are unfavorable prognostic markers in low-grade glioma and glioblastoma multiforme. *Transl. Cancer Res.* **8**, 821–827 (2019).
37. Seifert, L. *et al.* The necrosome promotes pancreatic oncogenesis via CXCL1 and Mincle-induced immune suppression. *Nature* **532**, 245–249 (2016).
38. Lomphithak, T. *et al.* Tumor necroptosis is correlated with a favorable immune cell signature and programmed death-ligand 1 expression in cholangiocarcinoma. *Sci. Rep.* **11**, 11743 (2021).
39. Wang, Y. *et al.* Necroptosis regulates tumor repopulation after radiotherapy via RIP1/RIP3/MLKL/JNK/IL8 pathway. *J. Exp. Clin. Cancer Res.* **38**, 461 (2019).
40. Mahmoud, S. M. *et al.* Tumor-infiltrating CD8+ lymphocytes predict clinical outcome in breast cancer. *J. Clin. Oncol.* **29**, 1949–1955 (2011).
41. Ru, B. *et al.* TISIDB: An integrated repository portal for tumor–immune system interactions. *Bioinformatics* **35**, 4200–4202 (2019).
42. Höckendorf, U. *et al.* RIPK3 restricts myeloid leukemogenesis by promoting cell death and differentiation of leukemia initiating cells. *Cancer Cell* **30**, 75–91 (2016).
43. Nugues, A. L. *et al.* RIP3 is downregulated in human myeloid leukemia cells and modulates apoptosis and caspase-mediated p65/RelA cleavage. *Cell Death Dis.* **5**, e1384–e1384 (2014).
44. Lim, J. H. *et al.* Low-level expression of necroptosis factors indicates a poor prognosis of the squamous cell carcinoma subtype of non-small-cell lung cancer. *Transl. Lung Cancer Res.* **10**, 1221–1230 (2021).
45. Chung, J. H. *et al.* Receptor-interacting protein kinase 3 as a predictive adjuvant chemotherapy marker after lung adenocarcinoma resection. *Ann. Transl. Med.* **7**, 42 (2019).
46. Wang, H. H. *et al.* Ablative hypofractionated radiation therapy enhances non-small cell lung cancer cell killing via preferential stimulation of necroptosis in vitro and in vivo. *Int. J. Radiat. Oncol. Biol. Phys.* **101**, 49–62 (2018).
47. Liu, Z. *et al.* Tumor necroptosis-mediated shedding of cell surface proteins promotes metastasis of breast cancer by suppressing anti-tumor immunity. *Breast Cancer Res.* **25**, 10 (2023).
48. Eil, R. *et al.* Ionic immune suppression within the tumour microenvironment limits T cell effector function. *Nature* **537**, 539–543 (2016).
49. Olivo Pimentel, V., Yaromina, A., Marcus, D., Dubois, L. J. & Lambin, P. A novel co-culture assay to assess anti-tumor CD8+ T cell cytotoxicity via luminescence and multicolor flow cytometry. *J. Immunol. Methods* **487**, 112899 (2020).
50. Zuo, Y.-H. *et al.* Tumor PKCδ instigates immune exclusion in EGFR-mutated non–small cell lung cancer. *BMC Med.* **20**, 470 (2022).
51. Sun, X. *et al.* Inhibition of c-MET upregulates PD-L1 expression in lung adenocarcinoma. *Am. J. Cancer Res.* **10**, 564–571 (2020).
52. Zhao, C., Su, C., Li, X. & Zhou, C. Association of CD8 T cell apoptosis and EGFR mutation in non-small lung cancer patients. *Thorac. Cancer* **11**, 2130–2136 (2020).
53. Jiang, L. *et al.* Continuous targeted kinase inhibitors treatment induces upregulation of PD-L1 in resistant NSCLC. *Sci. Rep.* **9**, 3705 (2019).

Acknowledgements

This work was supported by grants from the Office of National Higher Education Science Research and Innovation Policy Council by Program Management Unit for Human Resources and Institutional Development, Research and Innovation (PMU-B; grant number B05F640067) to S.J.; the 90th Anniversary Chulalongkorn University Fund (Ratchadaphiseksomphot Endowment Fund; GCUGR1125632121M) and the National Research

Council of Thailand (NRCT) for graduate thesis to N.D. N.D. would like to thank the scholarship from the Graduate School, Chulalongkorn University to commemorate the 72nd anniversary of his Majesty King Bhumibol Adulyadej and Overseas Research Experience Scholarship for Graduate Student, Chulalongkorn University.

Author contributions

N.D. performed most of the experiments including IHC staining, analyzed all IHC data, and statistical analysis, organized the figures and drafted the manuscript under the supervision of S.J. T.L. performed in vitro experiments with T cells and drafted the manuscript under the supervision of S.J. R.S. analyzed most of IHC data. R.S. and J.A. provided NSCLC clinical data. Y.M. and C.I. helped with IHC staining. E.M. and I.S. provided NSCLC clinical samples. H.S. provided NSCLC clinical samples and revised the manuscript. S.J. conceived and designed the experiments, analyzed and interpreted the data and wrote the manuscript. All authors read and approved the final version of the manuscript.

Funding

The Office of National Higher Education Science Research and Innovation Policy Council by Program Management Unit for Human Resources and Institutional Development, Research and Innovation (PMU-B; grant number B05F640067); the 90th Anniversary Chulalongkorn University Fund (Ratchadaphiseksomphot Endowment Fund; GCUGR1125632121M); the National Research Council of Thailand (NRCT) for graduate thesis.

Competing interests

The authors declare no competing interests.

Ethical approval

Approval of the research protocol by an Institutional Reviewer Board: The study protocol was approved by the Ethics Committee at the Tohoku University School of Medicine and the Institutional Review Board of Thai Red Cross Society (IRB approval No. 7/2566).

Informed consent

All informed consent was obtained from the subject(s).

Additional information

Supplementary Information The online version contains supplementary material available at https://doi.org/10.1038/s41598-024-72545-2.

Correspondence and requests for materials should be addressed to S.J.

Reprints and permissions information is available at www.nature.com/reprints.

Publisher's note Springer Nature remains neutral with regard to jurisdictional claims in published maps and institutional affiliations.